

Adaptation to a new environment allows cooperators to purge cheaters stochastically

Adam James Waite^{a,b,1} and Wenying Shou^{b,1}

^aMolecular and Cellular Biology Program, University of Washington, Seattle, WA 98195; and ^bDivision of Basic Sciences, Fred Hutchinson Cancer Research Center, Seattle, WA 98109

This Feature Article is part of a series identified by the Editorial Board as reporting findings of exceptional significance.

Edited by Herbert Levine, University of California at San Diego, La Jolla, CA, and approved September 5, 2012 (received for review June 14, 2012)

Cooperation via production of common goods is found in diverse life forms ranging from viruses to social animals. However, natural selection predicts a “tragedy of the commons”: Cheaters, benefiting from without producing costly common goods, are more fit than cooperators and should destroy cooperation. In an attempt to discover novel mechanisms of cheater control, we eliminated known ones using a yeast cooperator–cheater system engineered to supply or exploit essential nutrients. Surprisingly, although less fit than cheaters, cooperators quickly dominated a fraction of cocultures. Cooperators isolated from these cocultures were superior to the cheater isolates they had been cocultured with, even though these cheaters were superior to ancestral cooperators. Re-sequencing and phenotypic analyses revealed that evolved cooperators and cheaters all harbored mutations adaptive to the nutrient-limited cooperative environment, allowing growth at a much lower concentration of nutrient than their ancestors. Even after the initial round of adaptation, evolved cooperators still stochastically dominated cheaters derived from them. We propose the “adaptive race” model: If during adaptation to an environment, the fitness gain of cooperators exceeds that of cheaters by at least the fitness cost of cooperation, the tragedy of the commons can be averted. Although cooperators and cheaters sample from the same pool of adaptive mutations, this symmetry is soon broken: The best cooperators purge cheaters and continue to grow, whereas the best cheaters cause rapid self-extinction. We speculate that adaptation to changing environments may contribute to the persistence of cooperative systems before the appearance of more sophisticated mechanisms of cheater control.

evolution of cooperation and cheating | experimental evolution | genetic hitchhiking | synthetic biology

The cooperative act of paying a cost to produce a publicly available good is a common biological phenomenon. Human volunteers contribute their time to build Wikipedia, which can be used by anyone with Internet access. Throughout the animal kingdom, alarm calls are produced by individuals to warn others of danger, even though producing the call makes the caller more conspicuous (1). Microbes excrete a plethora of costly compounds that can be used by the producers and their neighboring cells to acquire nutrients that are hard to obtain, access favorable environments, or improve antibiotic resistance (2, 3). In biological systems, publicly available goods are generally “common goods,” because consumption by one individual reduces their availability to others. “Cheaters” use the common good without paying a cost to produce it. Thus, because the common good is equally accessible to all members of a population, cheaters, introduced through migration or mutation, will be more fit than cooperators, increase in frequency, and eventually exhaust the common good, leading to the “tragedy of the commons” (4). For instance, although cooperative viruses produce diffusible shared proteins required for viral reproduction, selfish viruses synthesize less but sequester more of these proteins and thereby displace cooperative viruses, lowering overall infectivity (5). Cancers, a leading cause of death globally (6), cheat by exploiting the common

good produced by normal cells that cooperate to form a functional human body.

Despite exploitation of common goods by naturally arising cheaters, cooperation persists (7–13). How does cooperation survive cheating? We first summarize mechanisms known to stabilize cooperation against cheating. We then describe our attempts to discover novel mechanisms of cheater control by excluding known ones from an engineered yeast cooperator–cheater system.

Frequently, through unexpected genetic or physical processes, what initially appear to be cheaters or common goods are not; thus, the tragedy of the commons does not apply. For instance, a gene required for cooperation can have pleiotropic effects, such that a cell defective in paying the cost of cooperation is also incapable of enjoying the cooperative benefit. In this case, cheaters will end up suffering a net fitness cost. This situation has been found to occur in the social amoeba *Dictyostelium discoideum*. *D. discoideum* responds to starvation by aggregating and forming a fruiting body. During fruiting body formation, some cells form a self-sacrificing, nonreproductive stalk, which lifts other cells that differentiate into reproductive spores. The gene encoding the receptor necessary for differentiation into stalk cells is also necessary for proper spore formation; thus, cheaters trying to avoid the stalk fate cannot become spores (14). Another possibility is that what appears to be a common good is actually partially privatized by its producer. For instance, the budding yeast *Saccharomyces cerevisiae* secretes invertase to hydrolyze the disaccharide sucrose into glucose and fructose, which can be metabolized more efficiently. These monosaccharides were initially thought to be strictly common goods (15), although it was later found that ~1% are retained by the producing cell (16). Even such a seemingly insignificant level of privatization can allow cooperators to invade a population of cheaters (16, 17). This could explain the coexistence of invertase-producing cooperative cells with nonproducing cheating cells in wild populations (7). The benefits of privatization can only be realized when all cooperators produce and consume the same common good (homotypic cooperation). In mutualism, privatization is pointless because each individual requires a common good produced only by its partners.

Even if cheaters have a net fitness advantage over cooperators that produce true common goods, several mechanisms can avert the tragedy of the commons. First, when individuals interact through the production and/or consumption of inexpensive common goods in randomly formed groups that assemble and

Author contributions: A.J.W. and W.S. designed research; A.J.W. performed research; A.J.W. contributed new reagents/analytic tools; A.J.W. and W.S. analyzed data; and A.J.W. and W.S. wrote the paper.

The authors declare no conflict of interest.

This article is a PNAS Direct Submission.

See Commentary on page 19037.

¹To whom correspondence may be addressed. E-mail: adam.james.waite@gmail.com or wenying.shou@gmail.com.

This article contains supporting information online at www.pnas.org/lookup/suppl/doi:10.1073/pnas.1210190109/-DCSupplemental.

disassemble cyclically, as long as an increase in the availability of the common good leads to a less than proportional increase in the fitness of its consumers, a stable equilibrium between cooperators and cheaters is expected (18, 19). This “diminishing return” of the common good (16, 18) can account for the surprising observation that in the yeast invertase system, maximum group size is attained with a mixture of cheaters and cooperators: Cooperators produce more invertase than they can use, and cheaters convert this excess benefit into additional biomass (20). The cost-to-benefit ratio can be kept low if the common good is produced facultatively (i.e., only when needed), which is the case for most organisms, or if the durability of common goods is high, as found in siderophore production in *Pseudomonas aeruginosa* (21, 22). Second, for cooperation based on scarce common goods, mechanisms of “positive assortment” that increase the frequency of interactions between cooperators (23) can facilitate the persistence of cooperation. Positive assortment can involve specifically directing benefits to other cooperators and excluding or punishing cheaters based on recognition or previous experience (24–26). This can occur even in organisms lacking nervous systems. For instance, microbes can achieve “recognition” through cell adhesion and chemical communication (27), and legumes “reward” and “punish” beneficial and cheating rhizobia, respectively (28, 29). Another mechanism of positive assortment is “population viscosity,” brought about by limited dispersal in spatially structured environments, which keeps cooperators clustered with their relatives in homotypic cooperation (24, 30–32), or with their partners in heterotypic cooperation (33). Thus, natural cooperative systems, whether homotypic or heterotypic, use many different mechanisms to mitigate the tragedy of the commons, allowing cooperation via common goods to be a successful evolutionary strategy.

Existing cooperative systems may have evolved for millions of years, and can now deploy mechanisms, such as pleiotropy, facultative production of common goods, and cheater recognition, to prevent destruction by cheaters. However, what about cheater control at the origins of these systems? A spatially structured environment can stabilize cooperation against cheating; however, under certain circumstances, it can hinder cooperation (34–36) through enhancing competition among cooperators (37–39). Furthermore, motile species may behave as if they were locally well-mixed even if they live in a spatially structured environment. To search for novel cheater-control mechanisms that might stabilize nascent cooperative systems, we extended a synthetically engineered model of cooperation (40) to include cheating (Fig. 1A). In this system, which is based on the yeast *S. cerevisiae*, cooperation occurs between the red-fluorescent $R_{\rightarrow A}^{-L}$ strain, which requires lysine ($\leftarrow L$) and provides adenine ($\rightarrow A$), and the yellow-fluorescent $Y_{\rightarrow L}^{-A}$ strain, which requires adenine ($\leftarrow A$) and provides lysine ($\rightarrow L$). The presence of both $R_{\rightarrow A}^{-L}$ and $Y_{\rightarrow L}^{-A}$ is necessary for growth in minimal media lacking adenine and lysine (SD) (40). The cheater is a cyan-fluorescent C^{-L} strain that requires lysine but does not provide any nutrients.

This system allows us to remove the mechanisms currently thought to avert the tragedy of the commons in a systematic manner. Engineering the cooperative interactions through mutations that constitutively overproduce metabolites eliminates the possibility of pleiotropy or facultative production. Using a two-partner heterotypic cooperative system renders privatization of common goods futile, because neither strain can directly use the common good it produces. After an initial period of asymmetrical nutrient release and cell death (40), our cooperative cocultures approach a stable doubling time (~ 12 h) that is much slower than those of the corresponding monocultures supplemented with the necessary nutrient (~ 2 h). Thus, common goods are very limited. Additionally, because cooperation is based on metabolic manipulations not found in the ancestor strain, it is unlikely that the cooperating partners could recognize one another or exclude the

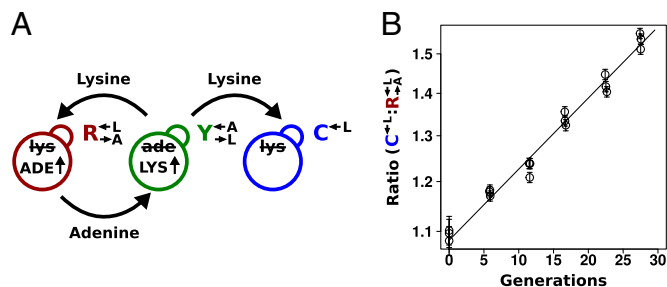


Fig. 1. (A) Yeast model of cooperation and cheating. Our cooperative system is composed of two nonmating yeast strains. The red-fluorescent $R_{\rightarrow A}^{-L}$ strain (WY950) requires lysine and overproduces adenine, whereas the yellow-fluorescent $Y_{\rightarrow L}^{-A}$ strain (WY954) requires adenine and overproduces lysine. The cheater is a cyan-fluorescent C^{-L} strain (WY962) that requires lysine and does not overproduce adenine. (B) Cheaters have a fitness advantage over cooperators. $R_{\rightarrow A}^{-L}$ and C^{-L} strains were mixed and competed in SD supplemented with nonlimiting (164 μ M) lysine. Cocultures were periodically diluted into fresh supplemented medium to maintain exponential growth. The ratio of C^{-L} to $R_{\rightarrow A}^{-L}$ was determined using flow cytometry. The ratio was fit using weighted nonlinear least-squares regression to the form $A \exp(rt)$, where A is the initial ratio, r is the cheater growth rate minus the cooperator growth rate, and t is time in generations of $R_{\rightarrow A}^{-L}$. Note the logarithmic y axis. C^{-L} has a 1.8% (95% CI: 1.6–1.9%) advantage over $R_{\rightarrow A}^{-L}$.

cheater. Because all strains are derived from S288C, which does not flocculate (41), growth in well-mixed liquid culture prevents spatial clustering. Using a simple, well-defined model (42) free of known mechanisms of cheater control, we hoped to discover new mechanisms that may stabilize cooperation against cheating.

Results

Cheaters Are Fitter Than Cooperators. Many biosynthetic pathways are regulated by end-product feedback inhibition (e.g., 43, 44), which suggests that metabolite overproduction carries an evolutionarily significant cost. To quantify the cost of adenine overproduction in our cooperative yeast system, we competed $R_{\rightarrow A}^{-L}$ with C^{-L} in SD supplemented with excess (164 μ M) lysine and found that the latter carried a fitness advantage of 1.8% [95% confidence interval (CI): 1.6–1.9%; Fig. 1B]. In the absence of lysine, which occurs during the prolonged delay in lysine release by $Y_{\rightarrow L}^{-A}$ (40), $R_{\rightarrow A}^{-L}$ and C^{-L} died at similar rates (95% CI of the difference in death rate: -0.003 to 0.0003 h^{-1} ; Fig. S1). In both conditions, the fitness difference between expressing CFP and DsRed is small. Given the overall fitness advantage of C^{-L} over $R_{\rightarrow A}^{-L}$, the futility of privatization and paucity of common goods, and the lack of genetic mechanisms for cheater control, we predicted that in a well-mixed environment, C^{-L} would increase in frequency and eventually destroy the cooperative system.

Cheaters Are Stochastically Purged from Cocultures. We experimentally tested the prediction of deterministic cheater dominance by mixing $R_{\rightarrow A}^{-L}$, $Y_{\rightarrow L}^{-A}$, and C^{-L} at a ratio of 1:1:1 in SD (Fig. 2). This master mix was split into replicate cocultures that were monitored for growth and diluted to ensure that nutrients other than adenine and lysine were never limiting (*Materials and Methods*). Surprisingly, within 50 generations, we observed a bifurcation in growth rates (Fig. 2B): Some cocultures were growing slowly or not at all (Fig. 2A, gray triangles), whereas others continued to grow (Fig. 2A, orange triangles) at rates very similar to cheater-free cocultures (Fig. 2A, black circles). At ~ 450 h, we quantified the frequency of each population in each coculture using flow cytometry (Fig. 2C). The slow-growing cocultures (Fig. 2C, gray) contained mostly dead or dying cells that had lost membrane integrity, and therefore reacted with the nucleic acid dye TO-PRO-3. The remaining live cells were predominantly C^{-L} (“cheater-dominated”). Furthermore, cheater takeover took much less time than

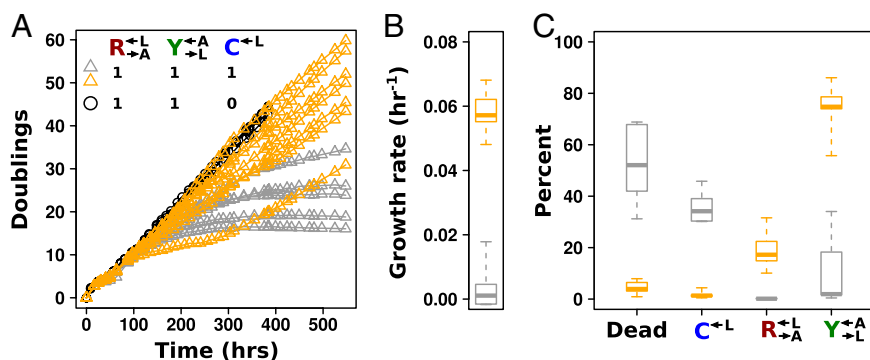


Fig. 2. Stochastic cheater outcome in initially identical cooperator–cheater cocultures. (A and B) Distinct growth behavior in replicate cooperator–cheater cocultures. Exponential cultures of $R_{\rightarrow A}^{-L}$, $Y_{\rightarrow L}^{+A}$, and C^{-L} were washed to remove residual supplements and mixed as indicated to a final density of 4.2×10^5 cells/mL per strain. Twelve plus-cheater (triangles) and three minus-cheater (black circles) cocultures were propagated, with total cell density maintained in the subsaturation range of $\sim 10^6$ cells/mL to 1.5×10^7 cells/mL by dilution into fresh SD when necessary. (B) After ~ 400 h, the growth rates of plus-cheater cocultures were bimodally distributed into fast-growing (orange) and slow-growing (gray) groups. (C) Fast-growing cocultures are dominated by cooperators. At ~ 450 h, the frequencies of dead cells reacting to the nucleic acid dye TOPRO-3 (Dead), C^{-L} , $R_{\rightarrow A}^{-L}$, and $Y_{\rightarrow L}^{+A}$ cells in fast-growing (orange) and slow-growing (gray) cocultures were quantified using flow cytometry. Boxes extend from the first quartile to the third quartile of the data, “whiskers” extend to the most extreme observations, and the thick bar inside each box represents the median.

predicted: In fewer than 40 generations, the average $C^{-L}/R_{\rightarrow A}^{-L}$ ratio was 280:1, as opposed to the 2:1 ratio predicted by the 1.8% fitness advantage of C^{-L} (Fig. 1B). Even more surprising were the fast-growing cocultures (Fig. 2C, orange). These cocultures contained mostly live $R_{\rightarrow A}^{-L}$ and $Y_{\rightarrow L}^{+A}$ cells (“cooperator-dominated”), with an average $R_{\rightarrow A}^{-L}/C^{-L}$ ratio of 16:1. We confirmed in subsequent experiments with a C^{-L} strain differentially marked with drug resistance that C^{-L} can be driven extinct in cooperator-dominated cocultures.

Extremely Fit Mutations Drive Stochastic Cooperator Dominance. To understand what had caused rapid divergence in population growth and stochastic cheater outcomes, we investigated the detailed population dynamics of these cocultures by frequently sampling replicate cocultures using flow cytometry. All $R_{\rightarrow A}^{-L}$ and C^{-L} populations, regardless of whether they eventually became cooperator- or cheater-dominated (Fig. 3A; solid or dashed lines, respectively), were nearly identical for the first ~ 60 h of growth, suggesting that the vast majority of cells were behaving identically and, most likely, ancestrally. Afterward, $R_{\rightarrow A}^{-L}$ and C^{-L} diverged rapidly (Fig. 3A). On the other hand, $Y_{\rightarrow L}^{+A}$ from cooperator-dominated and cheater-dominated cocultures behaved identically until after the divergence between $R_{\rightarrow A}^{-L}$ and C^{-L} (>80 h; Fig. 3A), suggesting that whatever was occurring in the $R_{\rightarrow A}^{-L}$ and C^{-L} populations preceded any changes in the $Y_{\rightarrow L}^{+A}$ population.

One possible explanation for the rapid population divergence was the presence of variants with large fitness advantages relative to their ancestor. Consider the cooperator-dominated coculture (Fig. 3A, solid lines). If the $R_{\rightarrow A}^{-L}$ population obtained the most fit variant ($R!$) by the time of population divergence (~ 60 h), $R!$ must have proliferated enough to influence the growth kinetics of the red-fluorescent population visibly. To estimate the fitness advantage of $R!$ over non- $R!$, we would need to know their relative abundance over time. We could not distinguish the two subpopulations directly from flow cytometry. However, because the $R_{\rightarrow A}^{-L}$ and C^{-L} populations initially behaved similarly, and we expected both to be influenced by the presence of $R!$ in a similar way, we assumed that the observed behavior of C^{-L} was similar to that of the non- $R!$ portion of the red-fluorescent population. Thus, the population size of $R!$ could be approximated by the difference between the red-fluorescent and cyan-fluorescent populations. Assuming that all $R!$ cells were descendants of a single cell present at the beginning of the experiment, this cell must

have doubled, on average, every ~ 3.4 h to achieve its estimated abundance at 80 h, a large improvement from the ancestral average doubling time of ~ 18.5 h (*Materials and Methods*). The same argument can be applied to the cheater-dominated coculture, which suggests that cooperation was destroyed by similar, highly adaptive variants that arose in the C^{-L} population. These variants must not have been rare (>1 in 10^6 cells), because, otherwise, in many cocultures, $R_{\rightarrow A}^{-L}$ and C^{-L} would have failed to sample any variant and population divergence would have been slow.

$R_{\rightarrow A}^{-L}$ and C^{-L} thus appeared to be engaged in an “adaptive race” to obtain the most fit variant. If the same pool of variants

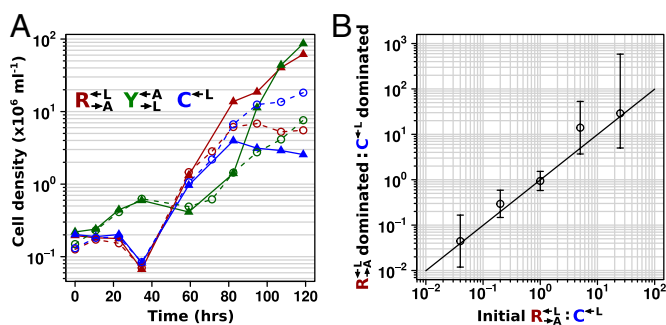


Fig. 3. (A) Rapid divergence in the growth of cooperators and cheaters in cooperator-dominated and cheater-dominated cocultures. Cocultures were initiated at a density of 1.7×10^5 cells/mL per strain. Cell densities of the three subpopulations were measured by flow cytometry by adding fluorescent beads of a known concentration to each sample. After initially following similar trajectories, rapid divergence resulted in dominance of $R_{\rightarrow A}^{-L}$ cells (triangles connected by solid lines) or C^{-L} cells (circles connected by dashed lines). A representative example of each class is shown. (B) Frequency of cooperator-dominated cocultures is determined by the initial frequency of cooperators. Cocultures were prepared as in A, except the initial density of C^{-L} or $R_{\rightarrow A}^{-L}$ was varied from 8.3×10^5 to 4.2×10^6 cells/mL per strain. Total initial population size influenced how quickly cocultures diverged but not the eventual frequency of cooperator-dominated cocultures. Error bars represent 95% CIs, assuming that the number of viable cocultures followed a binomial distribution with parameters n and p , where n is the total number of cocultures and p is the probability of being cooperator-dominated. The slope of the logistic regression fitting line, $\log(\frac{p}{1-p}) = \beta \log(\frac{c}{1-c})$, where c is the initial cooperator frequency, is 1.0 (95% CI: 0.7–1.3). This suggests that the odds of being a cooperator-dominated coculture are nearly equal to the initial proportion of $R_{\rightarrow A}^{-L}$. This occurs because, in our system, the fitness cost of cooperation is small.

was sampled by both populations, the final ratio of cooperator-dominated/cheater-dominated cocultures should be determined by the initial ratio of $R_{\rightarrow A}^{-L}/C^{-L}$. Furthermore, in our system, these two ratios should be approximately equal because the fitness advantage of C^{-L} over $R_{\rightarrow A}^{-L}$ is insignificant compared with the fitness gain of a successful variant. We tested this idea by setting up cocultures at different initial ratios of $R_{\rightarrow A}^{-L}/C^{-L}$ (Fig. 3B; $R_{\rightarrow A}^{-L}/Y_{\rightarrow L}^{-A}$ was always 1:1). The slope relating the two ratios was 1.0 (95% CI: 0.7–1.3). Thus, consistent with our hypothesis that $R_{\rightarrow A}^{-L}$ and C^{-L} were sampling from the same pool of variants, the frequency of being cooperator-dominated was determined by the initial frequency of $R_{\rightarrow A}^{-L}$.

We next examined whether the improved fitness of these variants in the context of cooperation and cheating was a heritable phenotype. We isolated $Y_{\rightarrow L}^{-A}$, $R_{\rightarrow A}^{-L}$, and C^{-L} clones from a cooperator-dominated coculture; grew them in monoculture in SD supplemented with adenine or lysine; washed them free of supplements; and mixed them 1:1:1. Like the parental coculture, all six cocultures became cooperator-dominated (Fig. 4A, ii), which was significantly more than what was observed for 1:1:1 all-ancestor cocultures (Fig. 4A, i; 6 of 6 vs. 31 of 64 cooperator-dominated; Fisher's exact test, $P < 0.03$). The isolated $Y_{\rightarrow L}^{-A}$ clone did not contribute to cooperator dominance (Fig. 4A, iii; 3 of 6 vs. 31 of 64 cooperator-dominated; Fisher's exact test, $P > 0.9$). This is consistent with the idea that, short of partner-specific recognition, any changes in $Y_{\rightarrow L}^{-A}$ would affect C^{-L} and $R_{\rightarrow A}^{-L}$ equally. On the other hand, we tested one $R_{\rightarrow A}^{-L}$ isolate from each of seven independent cooperator-dominated cocultures and found that they dominated ancestral C^{-L} in a nearly deterministic fashion (Fig. 4A, iv; 41 of 42 vs. 31 of 64 cooperator-dominated; Fisher's exact test, $P < 3 \times 10^{-8}$). We then tested five isolates of C^{-L} from three independent cheater-dominated cocultures and found that they deterministically dominated ancestral cooperators (Fig. 4A, vii; 0 of 48 vs. 31 of 64 cooperator-dominated; Fisher's exact test $P < 10^{-9}$). Thus, changes occurring in $R_{\rightarrow A}^{-L}$ and C^{-L} were heritable and sufficient for dominating ancestral C^{-L} and $R_{\rightarrow A}^{-L}$, respectively.

If $R_{\rightarrow A}^{-L}$ and C^{-L} sampled from the same pool of mutations during the adaptive race, then even the "losing" types (i.e., $R_{\rightarrow A}^{-L}$ from cheater-dominated and C^{-L} from cooperator-dominated cocultures) may nevertheless have improved relative to their respective ancestors. We tested two losing C^{-L} isolates from cooperator-dominated cocultures, and both were significantly

better than ancestral C^{-L} at dominating ancestral $R_{\rightarrow A}^{-L}$ (Fig. 4A, v; 0 of 12 vs. 31 of 64 cooperator-dominated; Fisher's exact test, $P < 0.002$). We tested one losing $R_{\rightarrow A}^{-L}$ isolate, and it was better than ancestral $R_{\rightarrow A}^{-L}$ at dominating ancestral C^{-L} (Fig. 4A, vi; 6 of 6 vs. 31 of 64 cooperator-dominated; Fisher's exact test, $P < 0.03$).

In addition to dominating ancestral C^{-L} and the evolved C^{-L} that they had raced against, evolved $R_{\rightarrow A}^{-L}$ strains improved in the sense that they lowered the minimal cell density required to initiate a viable cooperative coculture (40). We tested a panel of six $R_{\rightarrow A}^{-L}$ strains isolated from cooperator-dominated or cheater-dominated cocultures. We mixed each isolate 1:1 with ancestral $Y_{\rightarrow L}^{-A}$ and serially diluted each coculture into SD. Compared with ancestral cocultures, cocultures initiated with evolved $R_{\rightarrow A}^{-L}$ required less than one-third of the initial cell density to achieve growth in 50% of replicate cocultures (Fig. 4B). Cocultures initiated with evolved $Y_{\rightarrow L}^{-A}$ showed a similar degree of improvement (Fig. S2).

The Adaptive Race Is Fueled by Mutations in a Small Set of Genes Involved in Nutrient Transport.

We used whole-genome resequencing to identify the mutations underlying the rapid evolution in cooperators and cheaters. Some strains contained only one unambiguous, high-quality, nonsynonymous SNP. These mutations defined a set of genes, exactly one of which was mutated in every sequenced strain that contained any nonsynonymous mutations. We therefore reasoned that mutations in these genes were responsible for improvements in cooperation and cheating relative to the ancestor strains. All alleles of these genes and the strains that contain them are reported in Table 1 (a complete list of sequenced strains and their SNPs can be found in Dataset S1). Of the 17 unique alleles found, *ECM21* and *DOA4* had 6 each, accounting for 70% of the total. A simple estimate based on the Poisson distribution suggests that we found ~97% of the genes responsible for the initial fitness increase. The small number of genes could still allow for rapid divergence between populations if each of the many alleles conferred a different fitness gain, because it would be unlikely for two populations to sample the same allele of the same gene.

Most of the identified genes suggested that evolved $R_{\rightarrow A}^{-L}$ and C^{-L} enhanced import of the limiting lysine provided by $Y_{\rightarrow L}^{-A}$ by decreasing transporter turnover. *Ecm21p* is an arrestin-like adaptor protein that allows the E3 ubiquitin ligase *Rsp5p* to ubiquitinate and degrade the high-affinity lysine permease *Lyp1p*

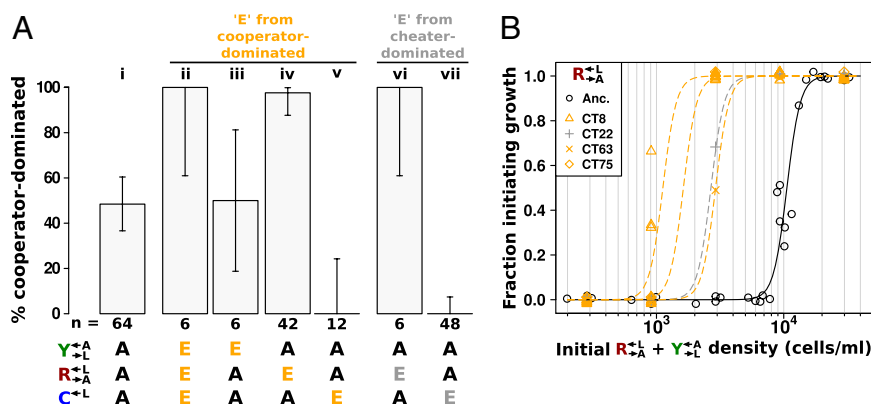


Fig. 4. Evolved cooperators and cheaters are superior to ancestors. (A) Improved cooperation and cheating are heritable and occur in both "winning" and "losing" strains. Cocultures consisting of ancestral strains (A) and strains isolated from cooperator-dominated (orange) or cheater-dominated (gray) cocultures (E) were formed as indicated at equal initial densities. Percentages of cooperator-dominated cocultures were measured from replicate cocultures whose numbers (n) are indicated. Error bars represent the 95% CI calculated as in Fig. 3B. (B) Improved $R_{\rightarrow A}^{-L}$ can initiate cooperation at lower densities than its ancestor. Ancestral $R_{\rightarrow A}^{-L}$ (black) and $R_{\rightarrow A}^{-L}$ isolated from cooperator-dominated (orange) and cheater-dominated (gray) cocultures were mixed 1:1 with ancestral $Y_{\rightarrow L}^{-A}$ and serially diluted into a microtiter plate. After 1 mo at 30 °C, wells showing visible growth were scored. Data are jittered slightly in the vertical direction to aid visualization.

Table 1. Mutations potentially sufficient for the observed large fitness advantage in the nutrient-limited cooperative environment

Gene	Allele	Strain	Cell type	Coculture dominated by	Mutant frequency
<i>ECM21</i>	Q143*	CT22	$R_{\rightarrow A}^{-L}$	Cheater	0.35
	E268*	CT11 [†]	C^{-L}	Cheater	
	S300*	CT78	$R_{\rightarrow A}^{-L}$	Cooperator	
	L475R	CT82	C^{-L}	Cheater	
	Q544*	CT65 [†] , CT75 [†]	$R_{\rightarrow A}^{-L}$	Cooperator	
	L780*	CT63 [†]	$R_{\rightarrow A}^{-L}$	Cooperator	
<i>DOA4</i>	D213G	CT60	$R_{\rightarrow A}^{-L}$	Cheater	0.35
	P235L	CT69, CT106	C^{-L}	Cheater	
	A643P	CT12	C^{-L}	Cheater	
	Q660K	CT7 [†]	$R_{\rightarrow A}^{-L}$	Cooperator	
	Ins 'A' → C735*	CT17	C^{-L}	Cooperator	
	Y916*	CT61 [†]	$R_{\rightarrow A}^{-L}$	Cooperator	
<i>RSP5</i>	L131W	CT8	$R_{\rightarrow A}^{-L}$	Cooperator	0.12
	N746K	CT110 [†]	C^{-L}	Cheater	
<i>BRO1</i>	Q434*	CT83 [†]	C^{-L}	Cheater	0.12
	S673*	CT57 [†]	$R_{\rightarrow A}^{-L}$	Cheater	
<i>LYP1</i>	D583N	CT10	C^{-L}	Cheater	0.06

Ins, indicates an insertion.

*Indicates STOP codon.

[†]Indicates the presence of additional high-quality SNPs in this strain.

in response to stress (45). All but one of the *ECM21* mutations introduced a premature stop codon before the PY-motif necessary for interaction with Rsp5p (45). Doa4p is a deubiquitination protein required to maintain free ubiquitin pools (46) and is specifically implicated in deubiquitination of plasma membrane proteins (47). Significantly, Doa4p represses expression of the general amino acid permease Gap1p (48), which can import lysine (49, 50). Less frequently observed were mutations in *RSP5* itself; in *BRO1*, which is necessary for the function of Doa4p by recruiting it to endosomes (51); and in the high-affinity lysine permease gene *LYP1* (50, 52).

To test whether nutrient transport was enhanced in evolved strains, we compared the ability of evolved and ancestral cells to grow into microcolonies (defined as >5 cells) under limiting concentrations of lysine. Although ancestral $R_{\rightarrow A}^{-L}$ and C^{-L} could grow on 4 μ M but not 1 μ M lysine (Fig. 5A, Anc.), every evolved $R_{\rightarrow A}^{-L}$ and C^{-L} isolate could grow as well on 1 μ M lysine as they did on 4 μ M lysine (Fig. 5A, Evo.). This improvement came at a cost, because almost all the evolved cooperators and cheaters grew slower in nonlimiting lysine than their ancestors (Fig. 5B), which is consistent with their low frequency at the start of our experiments. Thus, adaptation to the nutrient-limited cooperative environment involved a tradeoff in fitness in non-limiting nutrient.

To confirm that the observed mutations were sufficient to improve growth on limiting lysine, we replaced full-length *ECM21* in ancestral $R_{\rightarrow A}^{-L}$ and C^{-L} with the truncated version found in the evolved $R_{\rightarrow A}^{-L}$ strain CT22 (Table 1). Indeed, nearly 100% of these cells were able to grow on media containing 1 μ M lysine (Fig. 5A, *ecm21*).

Improved Cooperators Can Stochastically Defeat Newly Arising Cheaters. If during adaptation to the nutrient-limited cooperative environment, the maximum fitness gain of cooperators exceeds that of cheaters by at least the cost of cooperation, cooperators will win the race (Fig. 2A), and eventually purge the inferior cheaters. However, a mutation could turn an evolved cooperator into a cheater, which would now be as well-adapted to the nutrient-limited cooperative environment as the cooperators, and would therefore rise in frequency. Because successive fitness gains during adaptation to the same environment are expected to decrease over time (53), we tested whether evolved

cooperators could stochastically dominate otherwise isogenic cheaters during a subsequent round of the adaptive race. We chose two improved cooperator strains (CT22 and CT75; Table 1) carrying different truncation alleles of *ECM21* and derived, via allele replacement, matched cooperators and cheaters marked by different drug resistances (2 independent pairs from CT22 and 1 pair from CT75; Table 1 and Table S1). As a control, similarly matched cooperators and cheaters were derived from ancestral $R_{\rightarrow A}^{-L}$ (Table S1, WY1356-WY1359).

As before, $R_{\rightarrow A}^{-L}$ and C^{-L} pairs were mixed with ancestral $Y_{\rightarrow L}^{-A}$ at a ratio of 1:1:1. The frequencies of each cell type were

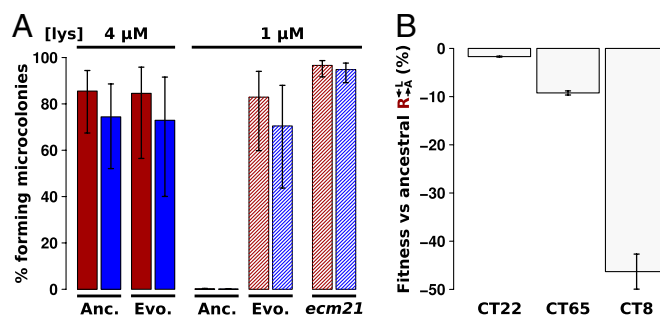


Fig. 5. Evolved cooperators and cheaters show a tradeoff between the ability to grow at low-lysine concentrations and the maximum growth rate achieved at high-lysine concentrations. (A) Evolved strains grow better at low-lysine concentrations than their ancestors. Exponentially growing ancestral (Anc.) or evolved (Evo.) cooperator (red) and cheater (blue) strains were washed free of lysine and starved for 16–20 h to deplete vacuolar storage of lysine. Cells were plated at ~ 200 cells/cm² onto minimal medium agar containing 4 μ M (solid bar) or 1 μ M (shaded bar) lysine. After 1–3 d, clusters of >5 cells were counted as microcolonies. Percentages and SEs were estimated using a generalized linear mixed-effect model (Materials and Methods). The *ecm21* ^{$\Delta 143$} allele from evolved cooperator CT22 was cloned into the ancestral cooperator and cheater strains (Materials and Methods), and their growth on low-lysine plates was measured (*ecm21*). The percentage is based on scoring >100 cells. Error bars indicate the 95% CI, assuming a binomial distribution with parameters n and p , as in Fig. 3B. (B) Evolved cooperators have lower growth rates than their ancestors in nonlimiting lysine. Relative fitness compared with ancestral $R_{\rightarrow A}^{-L}$ was measured for CT22 and CT65 through direct competition and calculated for CT8 using monoculture growth rates.

periodically measured by plating onto media containing the appropriate antibiotic. As expected, the derived ancestral cocultures showed stochastic cooperator dominance (2 of 12 were cooperator-dominated). Of the cocultures derived from the two *ecm21* alleles (Fig. 6, *ecm21*^{+L}_{-A} and *ecm21*^{-L}), 11 were cooperator-dominated, 4 were cheater-dominated, and 2 were indeterminate. Thus, even after cooperators had obtained major fitness improvements in the cooperative environment, a fraction of them were able to fend off cheaters that were just as well-adapted.

Discussion

To uncover novel mechanisms that allow cooperation based on the production of common goods to survive cheating, we examined an engineered cooperative system that bypasses known mechanisms of cheater control. After adding cheaters, we expected slow but deterministic cheater takeover. Instead, identically initiated cocultures showed rapid population divergence: Whereas cheaters rapidly destroyed cooperation in some cocultures, cooperators rapidly displaced cheaters in other cocultures. We determined that this process was an adaptive race between cheaters and cooperators that was driven by strong selection for improved growth in the novel, nutrient-limited cooperative environment.

The race between cooperators and cheaters to adapt to a new environment can eventually favor cooperation, despite the initial fitness advantage of cheaters. As has been shown theoretically, if the frequency of recombination is negligible and if the fitness gain of the most adaptive mutation in cooperators exceeds that of cheaters by at least the fitness cost of cooperation, the cooperative trait can “hitchhike” on environmental adaptation and rise to high frequency (54–56). Otherwise, cheaters dominate. Thus, the probability of either type eventually dominating a coculture is related to its initial abundance in the population (Fig. 3B), because a larger population is more likely to sample better mutations. However, this initial symmetry is quickly broken: If cheaters dominate, the cooperative system will collapse (Fig. 2, gray) because the common good necessary for survival is no

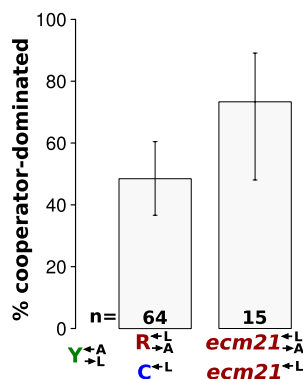


Fig. 6. Stochastic cheater purging observed in cocultures composed of cooperators and cheaters previously exposed to the cooperative environment. We replaced the adenine overproduction allele of *ADE4* (*PUR6*) in two evolved *R*_{-A}^{+L} strains containing truncation alleles of *ECM21* (CT22 and CT75; Table 1) with *PUR6* or WT *ADE4* marked with different antibiotic resistances. Cocultures were initiated at 1:1:1. Frequencies of cell types were periodically determined by plating onto media containing the appropriate antibiotic. A coculture was considered “cooperator-dominated” if the ratio of *R*_{-A}^{+L} to *C*^{-L} was >100, or if the frequency of *C*^{-L} fell below 1% of its initial frequency. It was considered “cheater-dominated” if the ratio of *C*^{-L} to *R*_{-A}^{+L} was >100, or if the frequency of *R*_{-A}^{+L} fell below 1% of its initial frequency. It was considered “indeterminate” if none of these conditions were satisfied after ~2,000 h of propagation. Indeterminate cocultures were excluded from the analysis. Because results across pairs were not significantly different from one another, the data were combined and are presented as *ecm21*_{-A}^{+L} and *ecm21*^{-L}. Error bars are the 95% CIs calculated as in Fig. 3B.

longer produced in sufficient quantities. In fact, the better the mutation obtained by cheaters, the sooner self-extinction will occur. On the other hand, if cooperators dominate, they continue to produce the common good and proliferate (Fig. 2, orange). These cooperators have improved their ability to initiate cooperation (Fig. 4B) and are able to defeat evolved cheaters that are superior to the ancestral cheater (Fig. 4A). While proliferating, cooperators can potentially acquire further beneficial mutations (57).

Two factors can synergize with the adaptive race to stabilize cooperation. First, different types of environmental change can provide different opportunities for adaptation. Improved cooperators that have survived one round of the adaptive race will eventually generate cheating mutants. Initially, the small population size of these cheating mutants makes them vulnerable to extinction by genetic drift and less likely to acquire the best mutation during subsequent rounds of the adaptive race. Eventually, however, cheaters will crash the cooperative system if the environment remains constant long enough. This is because the magnitude of possible fitness gains from subsequent adaptations will diminish over time (53). However, other environmental changes in, for example, temperature or osmolarity will select for distinct mutations that confer large fitness gains, triggering another adaptive race. Second, if individuals can migrate between spatially separated populations, “Simpson’s paradox” allows cooperators to dominate globally even though cheaters grow faster in each population. This can occur even when the population structure is periodically destroyed by global mixing (58). The only requirement is sufficiently variable cheater frequency between groups, which can be achieved through dilution (58), or through mutations obtained during an adaptive race. Thus, in conjunction with spatially structured environments that change in different ways, two unavoidable realities of nature, the adaptive race “buys time” for a cooperative system to acquire additional mutations that may result in more reliable mechanisms of cheater tolerance, such as partner recognition.

Our cooperative system was engineered to cooperate in a manner completely foreign to its ancestor; thus, it is pertinent to consider whether the adaptive race occurs in more natural systems. We consider two examples in natural microbial cooperative communities in which the adaptive race may have operated. The first example involves the social bacterium *Myxococcus xanthus*, members of which, when starved, exchange developmental signals, aggregate, and differentiate to form a fruiting body. During this process, a majority of cells die, whereas the remaining cells become tough spores (59). This provides an opportunity for a strain to cheat by disproportionately forming spores when mixed with another strain (60). One cheater strain that could not form spores on its own repeatedly rose to a high frequency when mixed with a cooperative strain and drove the entire system to very low population sizes (60). Reminiscent of our system, some of the replicate cocultures suffered complete collapse, whereas the remaining cocultures emerged cheater-free. If not solely due to drift, we suspect that this stochastic cheater outcome may be the result of an adaptive race similar to what we report here. This could occur if the cheater created a novel environment unfamiliar to the cooperative ancestor strain. If the emerging cooperators demonstrate an improved ability to defeat ancestral cheaters, sequencing evolved cooperators might reveal the type of novel environment imposed by cheaters, as well as the mechanisms deployed to adapt to it.

A second example of a potential adaptive race was recently shown in the siderophore-producing bacterium *Pseudomonas fluorescens* (54). During iron limitation, *P. fluorescens* produces and releases iron-chelating siderophores that can be taken up by any nearby individual. When nonproducing cheaters, which have a large fitness advantage over siderophore-producing cooperators, were mixed with cooperators in an iron-limited environment, cheaters introduced at low frequency failed to invade (61). The authors proposed that this occurred because the numerically

dominant cooperators had a greater chance of obtaining a high-fitness mutation adaptive to iron limitation that could sweep through the population. However, the actual mechanisms were not determined. This implies that although *P. fluorescens* must have experienced similar types of iron limitation throughout its evolutionary history, as evidenced by the very existence of siderophore production, the experimentally imposed iron limitation was still sufficiently “novel” to elicit an adaptive race. This supports our experimental finding that the environment does not need to be completely novel for the adaptive race to occur (Fig. 6).

Similar genetic hitchhiking in a not-so-novel environment was recently observed outside the context of cooperation. In an experiment initially designed to track deterministic takeover of sterile yeast mutants (which have greater fitness than nonsterile cells), the researchers observed complex patterns consistent with the rise of multiple nonsterile mutants with greater fitness than the sterile mutants (62). Importantly, this occurred in rich media thought to impose minimal selective pressure. These examples illustrate that the conditions necessary to initiate the adaptive race may be met more frequently than is currently assumed.

In summary, by using an engineered cooperating–cheating yeast system to bypass all known cheater-control mechanisms, we discovered that the adaptive race allowed cooperators to defeat cheaters stochastically. This simple mechanism requires low rates of recombination and can be triggered by any environment in which adaptation offers fitness gains greater than the cost of cooperation. Experimental evidence from naturally occurring cooperative systems suggests that these conditions may be met even when the environment is not completely novel (60, 61). Because adaptation to a changing environment is the norm in biology, we propose that the adaptive race between cooperators and cheaters, especially in spatially structured populations, is a fundamental mechanism for cooperative systems to survive the perpetual onslaught of cheaters.

Materials and Methods

Strains and Cell Culture. All strains were derived from the BY designer deletion strains of the S288C background (63) and created essentially as described by Shou et al. (40). A list of constructed strains used in this study is provided in Table S1. To derive cooperating and cheating strains from a parent strain, DNA fragments PCR-amplified off a cassette containing either WT *ADE4* and resistance to Hygromycin B (*hph*; WSB150) or an *ADE4* overproduction allele (*PUR6*) and resistance to ClonNAT (*nat*; WSB151) were transformed into the parent strain. The primers contained regions homologous to the site of integration. Transformants were selected on media containing the appropriate antibiotic. The presence of *ADE4* or *PUR6* in the lysine-auxotrophic parent strain was determined by patching a small amount of transformant onto SD + lysine plates prespread with *ade8* diploid cells and cut into individual squares. Overproduction of adenine resulted in adenine release and visible growth of *ade8* cells into satellite colonies, whereas strains with *ADE4* did not. By replacing *ECM21* after the 142nd amino acid with DNA fragments PCR-amplified off an *hph*-containing cassette (WSB117), *ecm21*^{Δ143} strains were created.

Cells were grown at 30 °C in the rich medium YPD [1% (wt/vol) Bacto-yeast extract, 2% (wt/vol) Bacto-peptone, 2% (wt/vol) dextrose, 2% (wt/vol) Bacto-agar] or the minimal medium SD [0.67% (wt/vol) Difco Yeast Nitrogen Base without amino acids, 2% (wt/vol) dextrose] with or without supplemented amino acids, as necessary (64). To prepare for use, strains were struck from the freezer and grown on YPD plates at 30 °C for 2–3 d. An individual colony was picked and grown at 30 °C in liquid YPD until saturated (1–3 d). Unless otherwise indicated, strains were diluted >1:1,000 into SD + lysine or adenine and grown for ~16 h to exponential phase (~2 × 10⁶–4 × 10⁶ cells/mL) before being assayed.

Calculation of Average Doubling Times. The average doubling times of R_{-A}^{-L} and R^L were calculated using the formula $\frac{t}{\log_2 \left(\frac{N(t)}{N(0)} \right)}$, where t is time in hours,

$N(0)$ is the population size at time 0, and $N(t)$ is the population size at time t .

Competition Assays. To measure the fitness difference between cooperators and cheaters (Fig. 1B), exponentially growing cells were washed and resuspended in SD, diluted to 1.7×10^5 cells/mL into SD (for death competition) or SD + 164 μM lysine (for growth competition) in triplicate, and incubated at 30 °C on a rotator. Growing cocultures were periodically diluted to maintain exponential growth, while keeping population size above 3×10^4 cells per strain. Ratios of the competing strains were determined by flow cytometry periodically. The relationship between the C^{-L}/R_{-A}^{-L} ratio and time in generations of $R_{-A}^{-L}(t)$ was fit to the form $\frac{C^{-L}}{R_{-A}^{-L}} = A \exp(rt)$ using the method of weighted nonlinear least-squares, where A is the initial ratio and r is the difference in Malthusian parameters between C^{-L} and R_{-A}^{-L} . Because the growth rate of any population (R_{-A}^{-L} here) is $\ln(2)$ per generation by definition, percent fitness advantage with respect to R_{-A}^{-L} was calculated as $r/\ln(2)$. To determine fitness differences between R_{-A}^{-L} and its evolved descendants (Fig. 5B), which were all red-fluorescent, an otherwise isogenic yellow-fluorescent Y_{-A}^{-L} strain was competed against each strain. The difference in fitness between Y_{-A}^{-L} and R_{-A}^{-L} (0.1%) was an order of magnitude less than the difference in fitness between R_{-A}^{-L} and the fastest growing evolved strain (1.7%, CT22).

Flow Cytometry. Population compositions were measured by flow cytometry using a FACSCanto II (BD Biosciences) or DXP10 (Cytek) with three lasers (405 nm, 488 nm, and 633 nm). If necessary, fluorescent beads of known concentration were added to determine cell densities. Data analyses were performed using FloJo (TreeStar) or custom software written in R (65) using the Bioconductor (66) packages flowCore (67), flowMeans (68), and flowViz (69).

Coculture Growth and Assay of Population Compositions. Exponentially growing cells were washed in SD and counted using a CoulterCounter Z2 (Beckman Coulter) or by flow cytometry. After counting, cells were diluted into SD and mixed. Then, 3-mL aliquots were put in 13-mm tubes and cultured on a rotator at 30 °C. OD₆₀₀ was monitored at least once a day using a Gensys 20 (Thermo Spectronic), and population compositions were determined by flow cytometry. To estimate densities and ratios for the *ecm21* strains (Fig. 6), cocultures were sampled into a microtiter plate and serially diluted in 10-fold steps from 1- to 10⁻⁴-fold using a multichannel pipette; spotted onto agar plates containing YPD, YPD + clonNAT (100 μg/mL), and YPD + Hygromycin B (200 μg/mL); and incubated at 30 °C for up to 7 d. Colony counts were used to calculate population sizes of the entire coculture (YPD), *ecm21*^{-L} (YPD + clonNAT), and *ecm21*^{-L} (YPD + Hygromycin B).

Viability Assay. Exponentially growing cells were washed free of supplements. Ancestral Y_{-A}^{-L} and ancestral and evolved R_{-A}^{-L} strains were mixed 1:1 and serially diluted in a deep multiwell trough (~10 mL per well) (Fig. 4B). Six or twelve 200-μL aliquots of each prepared density were transferred into wells of a microtiter plate using a multichannel pipette, which were then sealed using parafilm and placed in a 30 °C incubator in moisturized Tupperware bins for 1 mo. Visible growth by eye was considered successful initiation of cooperation. Data were analyzed using a generalized linear model with a binomial link function. Strain and the logarithm of cell density were fixed effects.

Microcolony Growth Assay. Exponentially growing cells were washed and resuspended in SD, and then diluted to ensure that they would remain at low density after residual growth. After starvation in SD for 16–20 h, cell density was estimated by OD₆₀₀, diluted to ~10⁴ cells/mL, and plated onto SD plus 4 μM or 1 μM lysine (Fig. 5A). Plates were observed using light microscopy under a 10× objective after 24 h (4 μM lysine) or 48 h (1 μM lysine). Clusters of five or more cells were considered microcolonies. Percentages and 95% CIs for the ancestor and evolved data in Fig. 5A were estimated by a generalized linear mixed-effect model with a binomial link function using the package lme4 (70). Cooperator/cheater (“type”), ancestor/evolved (“state”), lysine concentration, and lysine concentration/state interaction were fixed effects, whereas strain and strain/experiment interaction were random effects.

Sequencing and Analysis. Genomic DNA was extracted using the Genomic-tip 20/G kit (QIAGEN). Libraries were prepared using the tagmentation reaction through the Nextera DNA Sample Preparation Kit, the Nextera Index Kit (96 indices), and TruSeq Dual Index Sequencing Primers (Illumina). All clean-up steps were performed with DNA Clean and Concentrator-5 (Zymo Research). Libraries from 30 strains (including the ancestral R_{-A}^{-L} and C^{-L}) were multiplexed and run on a HiSeq2000 (Illumina) using 50-cycle paired-end reading. Sequence data were analyzed using a custom Perl script that incorporated the bwa aligner (71) and SAMtools (72).

ACKNOWLEDGMENTS. We thank Justin Burton, who initially observed stochastic cheater outcomes; Wayne Gerard for performing the experiment used to generate Fig. 3A; Aric Capel for assistance with strain construction; Sarah Holte for help with statistical analysis; and Andy Marty and Ryan

Basom for help with sequencing. Work in the W.S. group is supported by the W. M. Keck Foundation, the National Institutes of Health (Grant 1 DP2 OD006498-01), and the National Science Foundation Bio/computation Evolution in Action Consortium (BEACON) Science and Technology Center.

1. Hollén LI, Radford AN (2009) The development of alarm call behaviour in mammals and birds. *Anim Behav* 78:791–800.
2. West SA, Diggle SP, Buckling A, Gardner A, Griffin AS (2007) The social lives of microbes. *Annu Rev Ecol Syst* 38:53–77.
3. Lee HH, Molla MN, Cantor CR, Collins JJ (2010) Bacterial charity work leads to population-wide resistance. *Nature* 467:82–85.
4. Hardin G (1968) The tragedy of the commons. *Science* 162:1243–1248.
5. Turner PE, Chao L (1999) Prisoner's dilemma in an RNA virus. *Nature* 398:441–443.
6. World Health Organization (2008) *The Global Burden of Disease: 2004 Update* (World Health Organization, Geneva) Available at: http://www.who.int/healthinfo/global_burden_disease/2004_report_update/en/index.html. Accessed May 22, 2012.
7. Naumov GI, Naumova ES, Sancho ED, Korhola MP (1996) Polymeric SUC genes in natural populations of *Saccharomyces cerevisiae*. *FEMS Microbiol Lett* 135:31–35.
8. Strassmann JE, Zhu Y, Queller DC (2000) Altruism and social cheating in the social amoeba *Dictyostelium discoideum*. *Nature* 408:965–967.
9. Schaber JA, et al. (2004) Analysis of quorum sensing-deficient clinical isolates of *Pseudomonas aeruginosa*. *J Med Microbiol* 53:841–853.
10. Dobata S, Tsuji K (2009) A cheater lineage in a social insect: Implications for the evolution of cooperation in the wild. *Commun Integr Biol* 2:67–70.
11. Vos M, Velicer GJ (2009) Social conflict in centimeter- and global-scale populations of the bacterium *Myxococcus xanthus*. *Curr Biol* 19:1763–1767.
12. Wilder CN, Allada G, Schuster M (2009) Instantaneous within-patient diversity of *Pseudomonas aeruginosa* quorum-sensing populations from cystic fibrosis lung infections. *Infect Immun* 77:5631–5639.
13. Jandér KC, Herre EA (2010) Host sanctions and pollinator cheating in the fig tree-fig wasp mutualism. *Proc Biol Sci* 277:1481–1488.
14. Foster KR, Shaulsky G, Strassmann JE, Queller DC, Thompson CRL (2004) Pleiotropy as a mechanism to stabilize cooperation. *Nature* 431:693–696.
15. Greig D, Travisano M (2004) The Prisoner's Dilemma and polymorphism in yeast SUC genes. *Proc Biol Sci* 271(Suppl 3):S25–S26.
16. Gore J, Youk H, van Oudenaarden A (2009) Snowdrift game dynamics and facultative cheating in yeast. *Nature* 459:253–256.
17. Doebeli M, Hauert C (2005) Models of cooperation based on the Prisoner's Dilemma and the Snowdrift game. *Ecol Lett* 8:748–766.
18. Foster KR (2004) Diminishing returns in social evolution: The not-so-tragic commons. *J Evol Biol* 17:1058–1072.
19. Archetti M, Scheuring I (2011) Coexistence of cooperation and defection in public goods games. *Evolution* 65:1140–1148.
20. MacLean RC, Fuentes-Hernandez A, Greig D, Hurst LD, Gudelj I (2010) A mixture of "cheats" and "co-operators" can enable maximal group benefit. *PLoS Biol* 8:e1000486.
21. Kümmerli R, Jiricny N, Clarke LS, West SA, Griffin AS (2009) Phenotypic plasticity of a cooperative behaviour in bacteria. *J Evol Biol* 22:589–598.
22. Kümmerli R, Brown SP (2010) Molecular and regulatory properties of a public good shape the evolution of cooperation. *Proc Natl Acad Sci USA* 107:18921–18926.
23. Fletcher JA, Doebeli M (2009) A simple and general explanation for the evolution of altruism. *Proc Biol Sci* 276:13–19.
24. Hamilton WD (1964) The genetical evolution of social behaviour. I. *J Theor Biol* 7:1–16.
25. Trivers RL (1971) The evolution of reciprocal altruism. *Q Rev Biol* 46:35–57.
26. Axelrod R, Hamilton WD (1981) The evolution of cooperation. *Science* 211:1390–1396.
27. Strassmann JE, Gilbert OM, Queller DC (2011) Kin discrimination and cooperation in microbes. *Annu Rev Microbiol* 65:349–367.
28. Kiers ET, Rousseau RA, West SA, Denison RF (2003) Host sanctions and the legume-rhizobium mutualism. *Nature* 425:78–81.
29. Heath KD, Tiffin P (2009) Stabilizing mechanisms in a legume-rhizobium mutualism. *Evolution* 63:652–662.
30. Maynard Smith J (1964) Group selection and kin selection. *Nature* 201:1145–1147.
31. Chao L, Levin BR (1981) Structured habitats and the evolution of anticompetitor toxins in bacteria. *Proc Natl Acad Sci USA* 78:6324–6328.
32. Nowak MA, May RM (1992) Evolutionary games and spatial chaos. *Nature* 359:826–829.
33. Harcombe W (2010) Novel cooperation experimentally evolved between species. *Evolution* 64:2166–2172.
34. Hauert C, Doebeli M (2004) Spatial structure often inhibits the evolution of cooperation in the snowdrift game. *Nature* 428:643–646.
35. Hansen SK, Rainey PB, Haagenen JA, Molin S (2007) Evolution of species interactions in a biofilm community. *Nature* 445:533–536.
36. Verbruggen E, et al. (2012) Spatial structure and interspecific cooperation: Theory and an empirical test using the mycorrhizal mutualism. *Am Nat* 179:E133–E146.
37. Queller DC (1992) Does population viscosity promote kin selection? *Trends Ecol Evol* 7:322–324.
38. West SA, Pen I, Griffin AS (2002) Cooperation and competition between relatives. *Science* 296:72–75.
39. Griffin AS, West SA, Buckling A (2004) Cooperation and competition in pathogenic bacteria. *Nature* 430:1024–1027.
40. Shou W, Ram S, Vilar JMG (2007) Synthetic cooperation in engineered yeast populations. *Proc Natl Acad Sci USA* 104:1877–1882.
41. Liu H, Styles CA, Fink GR (1996) *Saccharomyces cerevisiae* S288C has a mutation in FLO8, a gene required for filamentous growth. *Genetics* 144:967–978.
42. Momeni B, Chen C-C, Hillesland KL, Waite A, Shou W (2011) Using artificial systems to explore the ecology and evolution of symbioses. *Cell Mol Life Sci* 68:1353–1368.
43. Armitt S, Woods RA (1970) Purine-excreting mutants of *Saccharomyces cerevisiae*. I. Isolation and genetic analysis. *Genet Res* 15:7–17.
44. Blickling S, Knäblein J (1997) Feedback inhibition of dihydrodipicolinate synthase enzymes by L-lysine. *Biol Chem* 378:207–210.
45. Lin CH, MacGurn JA, Chu T, Stefan CJ, Emr SD (2008) Arrestin-related ubiquitin-ligase adaptors regulate endocytosis and protein turnover at the cell surface. *Cell* 135:714–725.
46. Swaminathan S, Amerik AY, Hochstrasser M (1999) The Doa4 deubiquitinating enzyme is required for ubiquitin homeostasis in yeast. *Mol Biol Cell* 10:2583–2594.
47. Dupré S, Haguenaer-Tsapis R (2011) Deubiquitination step in the endocytic pathway of yeast plasma membrane proteins: Crucial role of Doa4p ubiquitin isopeptidase. *Mol Cell Biol* 31:4482–4494.
48. Springael JY, Galan JM, Haguenaer-Tsapis R, André B (1999) NH4+–induced down-regulation of the *Saccharomyces cerevisiae* Gap1p permease involves its ubiquitination with lysine-63-linked chains. *J Cell Sci* 112:1375–1383.
49. Grenson M, Hou C, Crabeel M (1970) Multiplicity of the amino acid permeases in *Saccharomyces cerevisiae*. IV. Evidence for a general amino acid permease. *J Bacteriol* 103:770–777.
50. Regenbergh B, Düring-Olsen L, Kielland-Brandt MC, Holmberg S (1999) Substrate specificity and gene expression of the amino-acid permeases in *Saccharomyces cerevisiae*. *Curr Genet* 36:317–328.
51. Luhtala N, Odorizzi G (2004) Bro1 coordinates deubiquitination in the multivesicular body pathway by recruiting Doa4 to endosomes. *J Cell Biol* 166:717–729.
52. Grenson M (1966) Multiplicity of the amino acid permeases in *Saccharomyces cerevisiae*. II. Evidence for a specific lysine-transporting system. *Biochim Biophys Acta* 127:339–346.
53. Lenski RE, Travisano M (1994) Dynamics of adaptation and diversification: A 10,000-generation experiment with bacterial populations. *Proc Natl Acad Sci USA* 91:6808–6814.
54. Morgan AD, Quigley BJ, Brown SP, Buckling A (2012) Selection on non-social traits limits the invasion of social cheats. *Ecol Lett* 15:841–846.
55. Santos M, Szathmáry E (2008) Genetic hitchhiking can promote the initial spread of strong altruism. *BMC Evol Biol* 8:281.
56. Smith JM, Haigh J (1974) The hitch-hiking effect of a favourable gene. *Genet Res* 23:23–35.
57. Schwilk DW, Kerr B (2002) Genetic niche-hiking: An alternative explanation for the evolution of flammability. *Oikos* 99:431–442.
58. Chuang JS, Rivoire O, Leibler S (2009) Simpson's paradox in a synthetic microbial system. *Science* 323:272–275.
59. Velicer GJ, Vos M (2009) Sociobiology of the myxobacteria. *Annu Rev Microbiol* 63:599–623.
60. Fiegna F, Velicer GJ (2003) Competitive fates of bacterial social parasites: Persistence and self-induced extinction of *Myxococcus xanthus* cheaters. *Proc Biol Sci* 270:1527–1534.
61. Morgan AD, Quigley BJ, Brown SP, Buckling A (2012) Selection on non-social traits limits the invasion of social cheats. *Ecol Lett* 15:841–846.
62. Lang GI, Botstein D, Desai MM (2011) Genetic variation and the fate of beneficial mutations in asexual populations. *Genetics* 188:647–661.
63. Brachmann CB, et al. (1998) Designer deletion strains derived from *Saccharomyces cerevisiae* S288C: A useful set of strains and plasmids for PCR-mediated gene disruption and other applications. *Yeast* 14:115–132.
64. Guthrie C, Fink GR, eds (1991) *Guide to Yeast Genetics and Molecular Biology* (Academic Press, San Diego).
65. R Core Team (2011) *R: A Language and Environment for Statistical Computing* (R Foundation for Statistical Computing, Vienna). Available at <http://www.R-project.org>. Accessed September 26, 2012.
66. Gentleman RC, et al. (2004) Bioconductor: Open software development for computational biology and bioinformatics. *Genome Biol* 5:R80.
67. Hahne F, et al. (2009) flowCore: A Bioconductor package for high throughput flow cytometry. *BMC Bioinformatics* 10:106.
68. Aghaeepour N, Nikolic R, Hoos HH, Brinkman RR (2011) Rapid cell population identification in flow cytometry data. *Cytometry A* 79(1):6–13.
69. Sarkar D, Le Meur N, Gentleman R (2008) Using flowViz to visualize flow cytometry data. *Bioinformatics* 24:878–879.
70. Bates D, Maechler M, Bolker B (2011) lme4: Linear mixed-effects models using Eigen and Eigen. Available at <http://CRAN.R-project.org/package=lme4>. Accessed September 26, 2012.
71. Li H, Durbin R (2009) Fast and accurate short read alignment with Burrows-Wheeler transform. *Bioinformatics* 25:1754–1760.
72. Li H, et al. 1000 Genome Project Data Processing Subgroup (2009) The Sequence Alignment/Map format and SAMtools. *Bioinformatics* 25:2078–2079.

Supporting Information

Waite and Shou 10.1073/pnas.1210190109

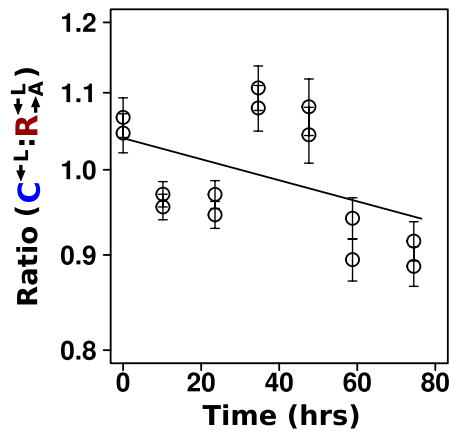


Fig. S1. Cheaters and cooperators die at similar rates. R_{-A}^{-L} and C^{-L} strains were mixed in minimal media that lack adenine and lysine (SD). The ratio of C^{-L} to R_{-A}^{-L} was determined using flow cytometry. The ratio was fit using weighted nonlinear least-squares regression to the form $A\exp(rt)$, where A is the initial ratio, r is the death rate difference of cheater over cooperator, and t is time in hours. Note the logarithmic y axis. No significant fitness difference was observed (95% confidence interval of difference in death rate: -0.003 to 0.0003 h^{-1}).

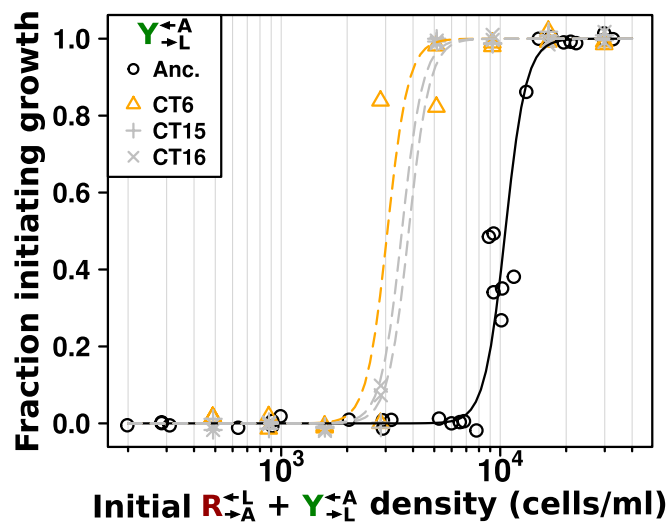


Fig. S2. Improved Y_{-L}^{-A} cooperators can also initiate cooperation at lower densities than their ancestors. Ancestral (Anc.) Y_{-L}^{-A} (black) and Y_{-L}^{-A} isolated from cooperator-dominated (orange) and cheater-dominated (gray) cocultures were mixed 1:1 with ancestral R_{-A}^{-L} and serially diluted into a microtiter plate. After 1 mo at 30 °C, wells showing visible growth were scored. Data are jittered slightly in the vertical direction to aid visualization.

Table S1. Constructed strains used in this study

Strain name	Derived from	Genotype
WY954 ($Y_{\rightarrow A}^{-L}$)		<i>MATa ste3::kanMX4 ade8Δ0 lys21::LYS21(fbr) trp1-289::pRS404(TRP1)-ADHp-Venus</i>
WY950 ($R_{\rightarrow A}^{-L}$)		<i>MATa ste3::kanMX4 lys2Δ0 ade4::PUR6 trp1-289::pRS404(TRP1)-ADHp-DsRed.T4</i>
WY962 ($C_{\rightarrow L}^{-L}$)		<i>MATa ste3::kanMX4 lys2Δ0 trp1-289::pRS404(TRP1)-ADHp-CFP</i>
WY1356, WY1357	WY962	<i>MATa ste3::kanMX4 lys2Δ0 ade4::TEFp-hph-TEFt-ADE4 trp1-289::pRS404(TRP1)-ADHp-DsRed.T4</i>
WY1358, WY1359	WY950	<i>MATa ste3::kanMX4 lys2Δ0 ade4::TEFp-nat-TEFt-PUR6 trp1-289::pRS404(TRP1)-ADHp-DsRed.T4</i>
WY1390	WY950	<i>MATa ste3::kanMX4 lys2Δ0 ade4::PUR6 trp1-289::pRS404(TRP1)-ADHp-DsRed.T4</i> <i>ecm21::ecm21^{Δ143}-loxP-hph-loxP</i>
WY1391	WY950	<i>MATa ste3::kanMX4 lys2Δ0 trp1-289::pRS404(TRP1)-ADHp-CFP ecm21::ecm21^{Δ143}-loxP-hph-loxP</i>
WY1403, WY1404 ($ecm21^{-L}$)	CT22	<i>MATa ste3::kanMX4 lys2Δ0 ade4::TEFp-hph-TEFt-ADE4 trp1-289::pRS404(TRP1)-ADHp-DsRed.T4</i> <i>ecm21^{Q143*}</i>
WY1405, WY1406 ($ecm21_{\rightarrow A}^{-L}$)	CT22	<i>MATa ste3::kanMX4 lys2Δ0 ade4::TEFp-nat-TEFt-PUR6 trp1-289::pRS404(TRP1)-ADHp-DsRed.T4</i> <i>ecm21^{Q143*}</i>
WY1407 [†] ($ecm21^{-L}$)	CT75	<i>MATa ste3::kanMX4 lys2Δ0 ade4::TEFp-hph-TEFt-ADE4 trp1-289::pRS404(TRP1)-ADHp-DsRed.T4</i> <i>ecm21^{Q544*}</i>
WY1408 [†] ($ecm21_{\rightarrow A}^{-L}$)	CT75	<i>MATa ste3::kanMX4 lys2Δ0 ade4::TEFp-nat-TEFt-PUR6 trp1-289::pRS404(TRP1)-ADHp-DsRed.T4</i> <i>ecm21^{Q544*}</i>

*Indicates STOP codon.

[†]Indicates the presence of additional high-quality SNPs in this strain.

Other Supporting Information Files

[Dataset S1 \(XLS\)](#)